



Quasi-static and dynamic characterization of polyurea microspheres reinforced polyurea matrix composite



Sophia Do, Sophia Stepp, George Youssef*

Experimental Mechanics Laboratory, Mechanical Engineering Department, San Diego State University, 5500 Campanile Dr., San Diego, CA 92182, United States

ARTICLE INFO

Keywords:

Polyurea
Polyurea microspheres
Polymer matrix composite
Polyurea composites
Mechanical properties

ABSTRACT

Polymer matrix composites currently have a wide range of applications in the aerospace, automotive, and biomedical industries. The specific strength and stiffness of this class of materials can easily be engineered; however, the enhanced strength and stiffness are highly dependent on the quality of the interfacial bonding between the reinforcement and matrix. It is thus the aim of this research to synthesize and characterize a polyurea matrix composite that is reinforced by polyurea microspheres to reduce the mechanical mismatch and improve bonding. For this composite, a hyper-viscoelastic polyurea formed from Versalink® P1000 and Isonate® 143 L, was chosen for its superior moisture resistance, and excellent thermal and impact mitigation properties. From the micro-scale mechanical characterization, the composite displayed a 23 % increase in elastic modulus compared to the bulk counterpart. As a result of the quasi-static mechanical characterization, it was found that the elastic moduli were comparable between the composite and the neat polyurea, but showed an increase in yield stress and decrease in the area under the stress-strain curve as well as the loss of strain at failure. Dynamic mechanical testing indicated the comparable time-dependent response of the composite and neat samples above glass transition (T_g), while displaying a difference below T_g .

1. Introduction

Composite materials provide an enormous technological advantage over homogenous or monolithic counterparts since the stiffness and strength properties can easily be tuned by selecting and adjusting the volume fraction of the constituents. Generally, composite materials consist of two or more constituents, namely the reinforcement and matrix phases. The constituents can be selected from any synthetic or natural class of materials, including metals, ceramics, or polymers to engineer the composite to meet specific property maps. Nonetheless, polymer matrix composites (PMC) occupy the largest market share in current engineering applications, such as in aerospace, construction, and biomedical industries [1–3]. For example, in fiber-reinforced PMCs, the stiff and strong fibers, continuous or discontinuous, provide the dominant share of the mechanical properties, while the polymer matrix acts as the stress transfer as well as the bonding media making the overall geometry [4]. The disparity of the mechanical properties between the fibers and the adjacent matrix plays a major role in the failure or degradation of the performance of PMCs. One major issue that arises from mechanical properties mismatch is delamination due to the stress build-up at the interface or generally in the inter-phasic region. A need, therefore, becomes apparent for a hybridization paradigm where

a reinforcement and matrix combination has a lower mechanical mismatch and a better bonding interface. Hence, the focus of the current research is to investigate the technological feasibility of a self-reinforcement polymer-polymer composite through the synthesis of stiffer and stronger particulates from the same matrix material in an attempt to overcome the mechanical mismatch dichotomy.

Polyurea, a versatile thermoset polymer with a wide variety of uses in both biomedical and industrial applications, is a promising matrix material for a PMC [5,6]. For the past two decades, polyurea has been heavily studied. Due to its chemical and moisture resistance, it is used as a sealant to protect structures, such as building roofs and water wells, from erosion and leakage [7–10]. Recently, polyurea is of interest for its ability to mitigate impacts, motivating its integration into protective armors for humans and structures [7–9,11]. Gupta et al. demonstrated the impact mitigating properties of polyurea by pioneering its integration into multiple civilian body armors including football helmets, running shoes, and hip protective pads. They reported ~20 % reduction in the probability of concussion in helmet-to-helmet impact scenarios, for example [8]. When used in conjunction with metal plates for armors, it was also found to alter the fragmentation behavior of the armor plates [12]. When polyurea was added, the armor plates displayed plastic bulging, rather than the traditional elastic failure with

* Corresponding author.

E-mail address: gyoussef@sdsu.edu (G. Youssef).

projectile shrapnel that is generally associated with standalone metal plates upon impact, thus protecting assets from secondary and tertiary impacts [7,11]. Similarly, adding polyurea coating on building foundation was found to adhere to the structure and remain intact during an explosion, inhibiting debris from being propelled by the blast thus reducing the severity of violent secondary and tertiary mechanical impacts [12]. Polyurea has also been shown to resist moisture and improve the fracture toughness of a submerged bonded joint; hence its use in marine applications [9]. While polyurea elastomers have been heavily investigated in the area of protection and mitigation, it appears that the existing structure becomes the limiting factor for further integration into new applications or improvement of those already used in. Efforts to expand these mechanical limits have been directed toward reinforcement using CNT, carbon black, and glass microballoons, but it was found that at best the properties remain unchanged [12,13]. The reason for the lack of evolution in the properties, even using a novel reinforcement strategy, is the disparity between the properties of the polyurea matrix and the reinforcement phase.

The geometry of the reinforcement phase can either be continuous such as fibers or discontinuous (e.g., particulates). The latter takes different form factors that range from microspheres to whiskers and even random geometric particulates, but can be mechanically treated using macromechanics as far as the particle size exceeds ~ 100 nm. There are several metallic and ceramics particulate reinforcements used in PMCs, including organic (natural or synthetic) and inorganics (metal and metal oxides) [14]. Recently, there has been an increase in interest for polymer microspheres made of thermosets and thermoplastics [14–17]. For example, Do reported a modified precipitation polymerization process for the synthesis of polyurea microspheres based on the same chemicals used for polyurea-based impact mitigating structures [16]. There were found to exhibit a unique set of physical and mechanical properties in comparison to polyurea microspheres synthesized by Xu et al. [17]. While the processing yield of polyurea microspheres fabricated by Do was substantially lower than Xu et al., it was reported to inherit the hydrothermal and mechanical properties of bulk polyurea while exhibiting a higher modulus. For instance, the hydrothermal response of polyurea microspheres mirrored its bulk counterpart while the former exhibited a textured surface. Using scanning electron and atomic force microscopies, Do reported a size distribution of 2.4 ± 2.9 μm and a microscale modulus of 114.75 ± 40.71 MPa, respectively. The modulus of polyurea microspheres is 418 % higher than bulk polyurea made of the same chemicals [16]. In all, the textured surface and increase in modulus in the newly synthesized polyurea microspheres are desirable physical and mechanical properties for the sought after reinforcement phase, where the textured surface is expected to improve bonding due to mechanical interlocking and the increase in modulus is poised to increase the overall stiffness of the composite. It is important to note that since both

the reinforcement and matrix phases are made of the same materials, the interface quality is further improved through chemical bonding in addition to mechanical interlocking.

The objective of this research was to reinforce a polyurea matrix with previously synthesized polyurea microspheres to create a polymer-polymer composite with distinctively different properties than that of the neat polymer. The experimental research presented herein benchmarks the mechanical properties of the newly fabricated composites with samples extracted from neat polyurea sheets produced using the same manufacturing techniques. The micrographic investigation, dynamic mechanical analysis, and quasi-static testing were used to elucidate the differences.

2. Experimental approach

2.1. Sample preparation

As discussed above, Do recently report a detailed procedure to fabricate polyurea microspheres using a modified precipitation polymerization process reporting that the microspheres exhibited an average diameter distribution of 2.4 ± 2.9 μm and exhibited an elastic modulus of 114.75 ± 40.71 MPa, four times higher than their bulk counterpart [16]. Do also reported the need for polyurea microspheres to be sonicated and suspended in acetone to avoid agglomeration, if these microspheres were to be used as a reinforcement phase in a polymer-polymer composite [16]. Hence, the typical manufacturing process of polyurea sheets was modified to account for the addition of the suspension solvent. A total of four polyurea sheets were fabricated: two Polyurea-Polyurea composite sheets (one 1 mm thick and one 4 mm thick sheets) and two neat polyurea sheets (1 mm thick and one 4 mm thick sheet each). The 1 mm thick sheets were fabricated to extract samples for micromechanical and dynamic mechanical characterizations, while the 4 mm thick sheets were for quasi-static mechanical testing.

The 1 mm thick Polyurea-Polyurea composite sheet was fabricated by mixing a 4:1 wt ratio of Versalink® P1000 (oligomeric diamine) and Isonate® 143 L (4,4' methylene diphenyl diisocyanate), respectively, as the polyurea matrix. Prior to gelling, the polyurea matrix was added to the acetone-microsphere solution in a 3:1 wt ratio of polyurea matrix to acetone, where the amount of microspheres suspended in acetone-microsphere solution is equivalent to 1 wt percent of the polyurea matrix. The mixture was then poured into a Teflon coated aluminum mold and left in ambient conditions for 48 h to evaporate the acetone. After which, it was cured at 80°C under vacuum for 24 h. This process is schematically summarized in Fig. 1. It is important to note that the issue of particle settling is negligible herein since (1) the microspheres were added to the polyurea matrix just prior to gelling; (2) the viscosity of the polymer was continually increasing as a result of the

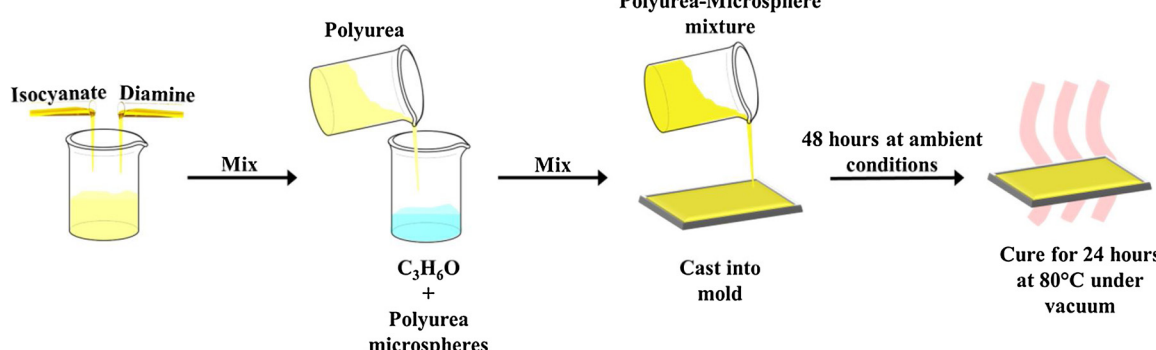


Fig. 1. Schematics of the fabrication process to cast a 1 mm nominal thickness Polyurea-Polyurea composite sheet by premixing diamine and isocyanate with 4:1 wt ratio with acetone-suspended polyurea microspheres that have an average diameter of 2.4 ± 2.9 μm . The casted sheet was cured in ambient laboratory conditions for 48 h to evaporate the acetone solvent and additional 24 h in a vacuum oven at 80°C .

polymerization process; and (3) the properties (e.g., density) of the microspheres and surrounding matrix were similar since they are made from the same polymer formulation.

Due to the usage of acetone to suspend and disperse the polyurea microspheres, difficulties arose when the previously mentioned process was repeated for the fabrication of the 4 mm thick sheet. The additional thickness of the sheet hindered the natural evaporation of acetone, causing through-thickness cracks in the sheet as the entrapped acetone vapor beneath the free surface increased the pressure between the mold surface and the hardened polyurea sheet. Thus, we had to modify the polyurea microspheres reinforced polyurea matrix composite fabrication process by reducing the amount of acetone and increasing the curing time in ambient conditions. For ease of sample release, the aluminum mold was also changed to a mold that was constructed of a polypropylene base and aluminum foil walls. The final process to fabricate the 4 mm thick Polyurea-Polyurea composite encompassed:

- (1) Mixing Versalink® P1000 and Isonate® 143 L in a 4:1 wt ratio, respectively;
- (2) The polyurea matrix was added to the acetone-microsphere solution in 8:2 wt ratio, respectively, with the amount of microspheres suspended in acetone-microsphere solution equivalent to 1 wt percent of the polyurea matrix before gelling; and
- (3) The sheet was then left to cure under ambient laboratory conditions for 5 days for natural acetone evaporation before curing at 80 °C under vacuum for an additional 24 h.

Sheets of neat polyurea without any reinforcement were also manufactured to quantitatively report the effect of reinforcing polyurea with the polyurea microspheres. To accurately report the effects of the reinforcement, the neat polyurea sheets were fabricated using the exact same process as their reinforced counterparts minus the addition and sonication of the microspheres. Once fabricated, the samples were die cut into dimensions required for each characterization step as seen in Fig. 2. As will be discussed next, the particle agglomeration was not found to be present in the final sample given the vigorous agitation before mixing as well as the chemical and hydrothermal stability of polyurea microspheres [16].

2.2. Characterization protocol

Microscale characterization was first done on the samples using scanning electron and atomic force microscopes. To expose the interface between the polyurea matrix and the polyurea microsphere reinforcement, a 1 mm thick with 25 mm diameter sample of the Polyurea-Polyurea composite was chilled below its glass transition

temperature using liquid nitrogen and fractured to expose a cross-section of the sample, which was then examined using a scanning electron microscope (SEM, FEI, Quanta 450). To explicate the micromechanical properties of the Polyurea-Polyurea composite, a disc sample with dimensions of 19 mm in diameter by 1 mm in thickness was tested using an Atomic Force Microscope (AFM, AFMWorkshop – TT2), where the sample was indented using a Bruker RTESPA-525 AFM tip at a loading rate of 5.7 nm.s^{-1} up to a maximum force of $\sim 2\mu\text{N}$ while measuring the indentation depth. The AFM investigation yielded a measure of the microscale elastic modulus [21], while providing an insight into the interaction between the polyurea reinforced microspheres and the surrounding matrix.

To elucidate the static and dynamic mechanical response of Polyurea-Polyurea composite in comparison to its neat counterpart, samples were extracted from the previously fabricated sheets and tested using a standard 1 kN load frame and a dynamic mechanical analyzer, both in tension, respectively. For the dynamic mechanical properties, both the Polyurea-Polyurea composite and neat polyurea sheets were die cut into dimensions of 33 mm long, 5 mm wide, and 1 mm thick samples and were tested using the film tension clamp in a dynamic mechanical analyzer (DMA, TA Instruments Q800). A total of 5 specimens from each sheet were individually secured into the clamps such that the sample had testing dimensions (i.e., the loaded section of the sample) of 18 mm long, 5 mm wide, and 1 mm thick. These sample dimensions were chosen to achieve a geometrical factor (GF) that fits within the operating range of the film tension clamp of the DMA based on the manufacturer and mechanics recommendations. The samples were then tested at different temperatures ranging from -100 °C to 50 °C with temperature steps of 10 °C. At each temperature step, the sample was held isothermally for 10 min to ensure that the entire sample had reached temperature prior to being stressed at a constant load of 0.5 MPa for 20 min while measuring the creep strain. The applied load of 0.5 MPa was chosen because it was previously determined to be well within the linear viscoelastic region for polyurea above its T_g of -49 °C [22]. The loading time period was chosen because a loading time of at least 3 decades (≥ 1000 s) is required to obtain the most data on the properties of the material [20] without crossing into the region of nonlinear stress-strain interdependence. The creep curves at each temperature step were then shifted using the Time-Temperature Superposition Principle to produce the master curve that displayed the long term dynamic properties of the samples, despite only testing each sample for a short period of time.

The quasi-static mechanical properties of both the homogeneous and composite sheets of polyurea were also tested in tension under ambient conditions using a 1 kN load frame (Instron 5843). A total of 5 samples were randomly extracted from each sheet using a hammer

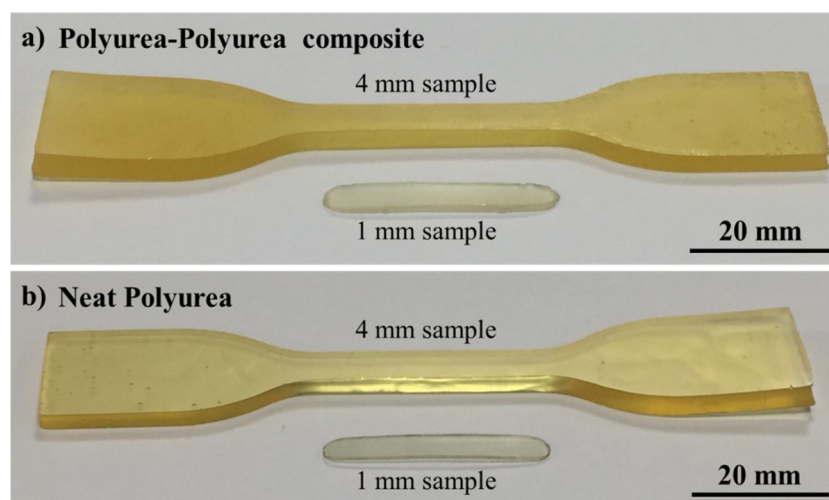


Fig. 2. Fabricated and die-cut samples for quasi-static and dynamic mechanical characterization of a) Polyurea-Polyurea composite and b) Neat Polyurea. The 4 mm-thick dog-bone samples were used for quasi-static testing while the 1 mm-thick strips were loaded in the dynamic mechanical analyzer. The selection of the samples geometry was based on the forecasted mechanical properties based on [18–20].

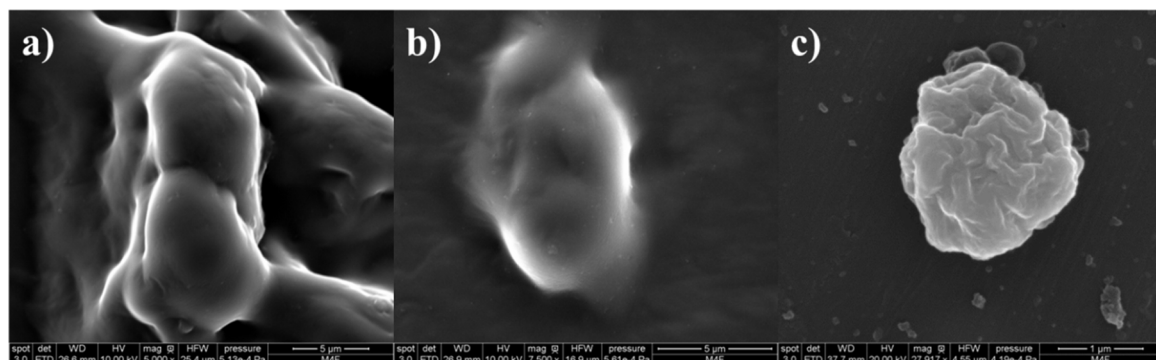


Fig. 3. Electron microscope micrographs of polyurea microspheres encapsulated in polyurea matrix from Polyurea-Polyurea composite sample that was chilled and randomly broken. SEM micrographs indicate dispersion of the microspheres as well as proper interfacial bonding while suggesting that the interfacial adhesion strength is superior to the matrix cohesion strength since there is no evidence of split microspheres.

punch die into ASTM D 638 Type IV specimen geometry. The samples were secured into the tension grips before being loaded at a rate of 50 mm.min⁻¹ until failure, while the resulting strain was measured using a high strain extensometer (Instron 2603 – 084). The stress and strain obtained from each of the samples were used to calculate the elastic modulus of the sample.

3. Results and discussion

The results and discussion section is divided into three subsections to mirror the steps discussed in the characterization protocol, where the results from the SEM and AFM investigations are first presented followed by the dynamic mechanical properties and the quasi-static response. In each of these sections, the properties and performance of the newly fabricated Polyurea-Polyurea composite were benchmarked with those of the neat polyurea.

3.1. Microscale characterization

The micrographs acquired using the scanning electron microscope (Fig. 3) support two overarching outcomes. First, the polyurea microspheres are well dispersed within the polyurea matrix as shown by the presence of multiple microspheres within the observed fracture surface, which was induced by randomly breaking a virgin, unloaded, and chilled polyurea sample as discussed above. The same observation is also consistent with the results of examining the fracture surface of mechanically loaded samples as discussed later. Fig. 3a shows two agglomerated polyurea microspheres while Fig. 3b shows a lone microsphere, where the microspheres are encased by the polyurea matrix in both cases. The dispersion of the microsphere is attributed to their suspension in an acetone solution and modifying the slab molding fabrication process to include the organic solvent as part of the mixture before curing. Moreover and because the microspheres and the surrounding media are made of the same materials, settling and buoyancy of the microspheres are not expected and shown to be negligible. Second, the SEM micrographs in Fig. 3a and b indicate the presence of a relatively thick polyurea matrix surrounding each of the microspheres. The rationale for the presumption about the thickness of the surrounding polyurea layer stems from the microscopic characterization of the standalone polyurea microspheres before the fabrication of the composite sheets. Do recently shown that the polyurea microspheres (Fig. 3c) used herein exhibit highly textured surfaces with crevices and grooves due to the drainage of solvents after the precipitation polymerization process during the dehydration stage [16]. In other words, the disappearance of the characteristic textures surface and the appearance of a relatively smooth surfaces point to good coverage of the polyurea matrix and bonding between the dispersed microspheres and the surrounding matrix.

In her study, Do also performed Fourier Transform Infrared Spectroscopy (FTIR) analysis on polyurea microspheres and affirmed the presence of unreacted and remnant isocyanate [16]. It is then believed that the remnant isocyanate on the surface of the microspheres promoted better adhesion at the interface as evident from the lack of visibility of interface between the microspheres and surrounding matrix. In essence, while breaking the chilled sample, the break-line appears to be trans-microspheres rather than inter-microspheres given the lack of evidence of any split spheres. It is important to note that the failure of the investigated polyurea-polyurea composite material is driven by the shear stresses in the material and most likely will always exhibit trans-microspheres breakage.

Prior to the nano-indentation study using the AFM, topographical scans of the samples surface were first obtained to clearly mark the area of investigation. This was followed by an indentation with approximately 2μN force while measuring the indentation depth to report the force-distance curve. Fig. 4a shows a typical topographical scan of the sample surface while Fig. 4b plots a typical force-displacement curve collected in response to indentation demonstrating the extend and retract phases on the test. Based on the analysis of the force-displacement curves, the indentation depth of the Polyurea-Polyurea composite and the neat polyurea were found to be 325 nm and 350 nm, respectively. Notably, the polyurea microspheres tested under the same conditions resulted in only 250 nm of indentation depth [16], which indicates the response of the composite sample is hinged on the properties of the reinforcement and matrix, and the volume of each. The relatively low indentation depth when testing the polyurea microspheres is also consistent with the disparity of the modulus between the microspheres and the bulk polyurea as noted by Do et al. [16]. In all, the average microscale elastic modulus of the Polyurea-Polyurea composite was reported to be 35.83 ± 12.78 MPa based on 27 indentations done at different locations of the sheet. The composite modulus was found to lie between that of polyurea microspheres (from Do et al. [16]) of 114.75 ± 40.71 MPa and the modulus of bulk polyurea of 27.44 ± 5.09 MPa. The method for deducing the microscale elastic modulus from the AFM force-displacement measurement has been recently reported in [21] based on the work of [23].

Based on micromechanical considerations, the elastic modulus of a composite should fall within the bounds of the Voigt upper limit and the Reuss lower limit depending on the volume fraction of reinforcement. The predicted elastic modulus for a 1 percent volume fraction of polyurea microspheres reinforcement would be 28.31 MPa and 27.65 MPa using the Voigt and Reuss models, respectively. However, the results reported above explicate that the measured elastic modulus of the newly synthesized Polyurea-Polyurea composite violates these predictions. This basically means that neither the state of deformation nor the state of stress is uniform throughout. The discrepancy between the theoretical predictions and our results is attributed to a twofold effect

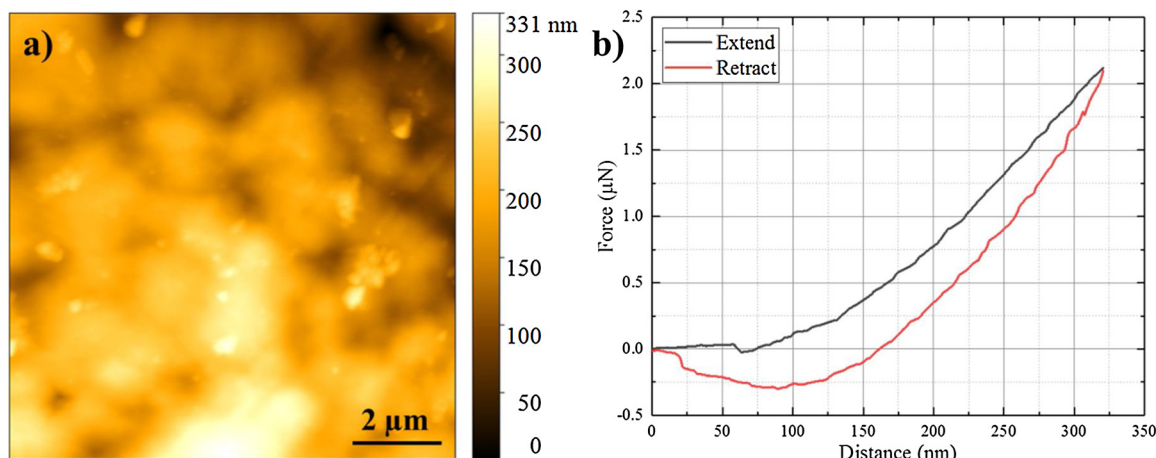


Fig. 4. (a) atomic force microscope topographical scans in the vicinity of the area where (b) AFM force-distance curve of Polyurea-Polyurea composite based on the application of $\sim 2\mu\text{N}$ force. The indentation depth for the Polyurea-Polyurea composite, Neat Polyurea, and polyurea microspheres was found to be 325 nm, 350 nm, and 250 nm, respectively.

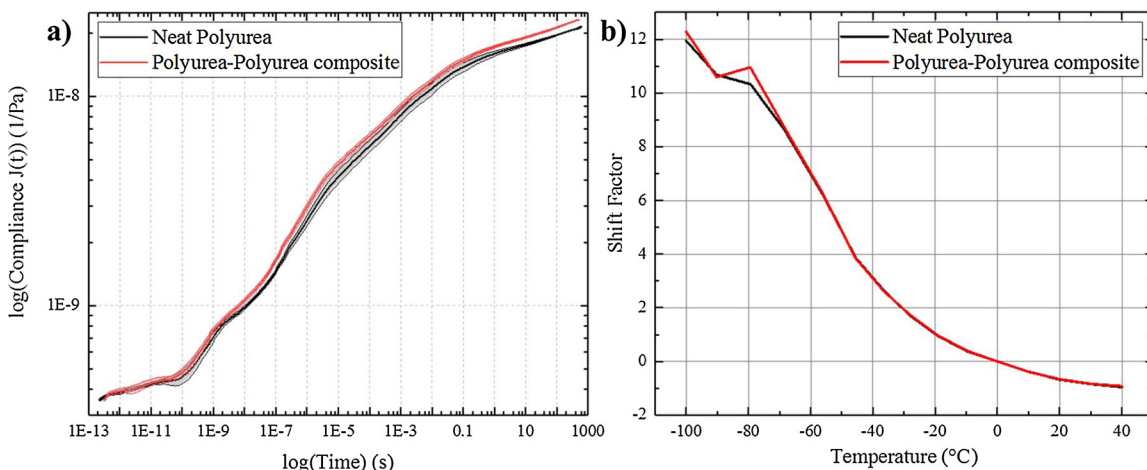


Fig. 5. Neat Polyurea and Polyurea-Polyurea composite a) master curves ($T_{\text{ref}} = 20$ °C) and the corresponding b) shift factors. The dynamic mechanical spectra were collected based on testing five samples at different temperatures ranging from -100 °C to 50 °C at constant stress of 0.5 MPa for 1200 s. The data was then shifted using Time-Temperature Superposition to yield the shown spectra.

that is not accounted for in Voigt or the Reuss models. First, the viscoelastic nature of polyurea is absent from these elastic models, which gives rise to time-dependent and strain-rate dependent responses. Second, the random dispersion of the microspheres in the matrix implies different mechanical interaction between the indenting AFM tip and the surface depending on the proximity of the spheres to the probed surface. The microspheres may be close to the surface or buried deep in the bulk of the matrix resulting from the mechanical mixing process during fabrication, which in turn yields different force-displacement data given the effect of the microspheres stiffness on the overall local response. It is well understood that the effect of the reinforcement phase is dependent of the concept of equivalent homogeneity as discussed by Christensen [24]. That is to say, the location of the reinforcing microspheres being at the surface, close to the surface, or deeply embedded into the matrix dictates the resulting mechanical stiffness. Accounting for the viscoelasticity of polyurea and the distribution of the microspheres (including the sphere-to-sphere interactions) are the focus of future research.

3.2. Dynamic mechanical response

The samples extracted from the 1 mm sheets were dynamically tested using a dynamic mechanical analyzer within the linear

viscoelastic regime, where each sample was characterized at a constant stress of 0.5 MPa for 1200 s at temperature steps ranging from -100 °C to 50 °C. The level of stress was defined based on a prior study by Whitten et al. to be within the linear viscoelastic regime [20]. The creep strain data at every temperature step was then shifted to produce a master curve as shown in Fig. 5a at a reference temperature of 20 °C. Fig. 5a included the average master curve for the composite and the neat samples based on average data collected from testing 5 different samples, which is represented by the solid red and black lines, respectively. The figure also includes a corresponding shaded area around each curve representing the standard error of the curve. As a result of the TTS shifting, Fig. 5b reports the averaged shift factor for each for the sample configuration. In general, the overall dynamic response appears to be nearly identical except for a slight increase in compliance, whereas the Polyurea-Polyurea composite exhibit 5.7 %, on average, increase over the entire range of time and temperature. The increase in mechanical compliance leads to the ascent in the level of deformation (discussed next) in response to the same levels of load, which indicates that the Polyurea-Polyurea composite may be suitable for impact mitigation applications given its potential ability to undergo more deformation than its neat counterpart. Moreover, the shift factor shows the same correspondence whether the microspheres were included or not, except at 80 °C and 100 °C. The obvious deviation in the response

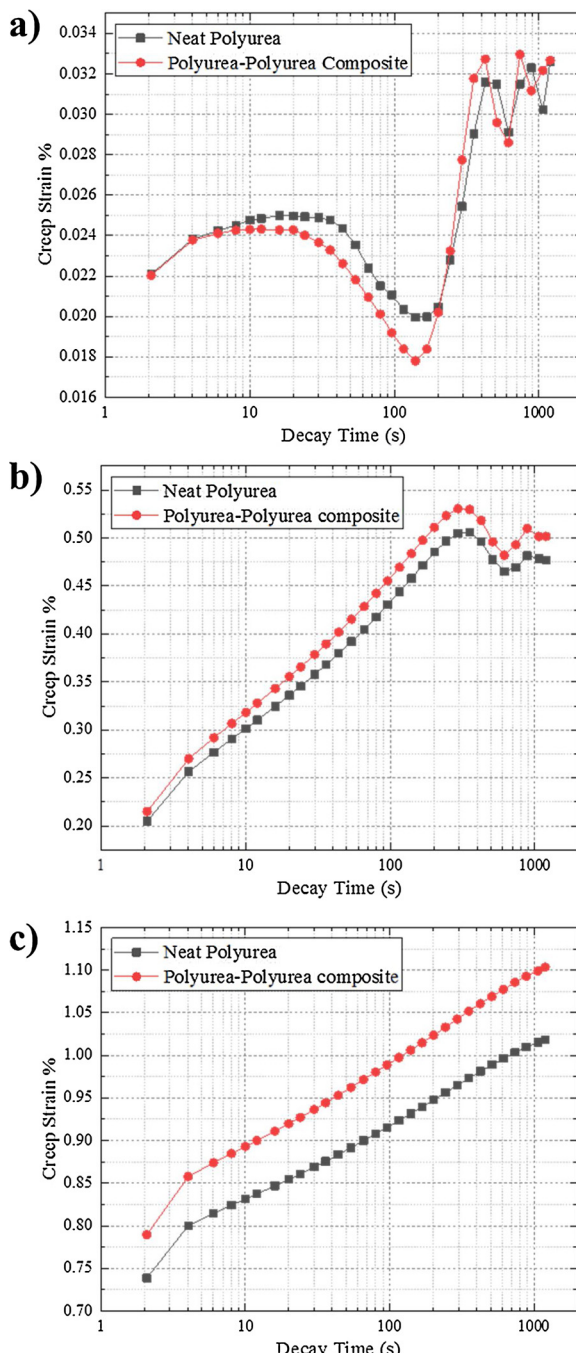


Fig. 6. Comparison of the creep strain over 1200 s at temperatures of a) -80 °C, b) -50 °C and c) 20 °C, which corresponds to the beta-transition, nearly at glass-transition, and at room temperature, respectively.

(also observable in the compliance-time master curve) might be associated with beta-transition, which is additional evidence of the suitability of the composite for mitigating impact loadings [25,26].

The aforementioned slight difference in the dynamic mechanical response can be more easily explicated by considering the creep strain as a function of testing time rather than the master curve. Fig. 6a-c shows the creep strain percentage as a function of the decay time, averaged from 5 samples, at selected temperatures of -80 °C, -50 °C and 20 °C, which were selected to correspond with beta-transition, nearly at glass-transition, and at room temperature, respectively. At -80 °C (Fig. 6a), the Polyurea-Polyurea composite appears to be slightly stiffer than the neat polyurea, where the strain percentage difference between

the two curves is ~4.6 %. As the samples are subjected to constant stress at a higher temperature near T_g as shown in Fig. 6b, the composite becomes more compliant than the neat counterpart, where the former strained 5.4 % more than the latter. As the temperature further increases to a temperature of 20 °C (Fig. 6c), the Polyurea-Polyurea composite becomes increasingly more compliant straining 7.8 % more than the neat polyurea. In all, the increase in strain in the Polyurea-Polyurea composite is indicative of the availability of more free volume in the continuum, which provides more space for the macromolecule to move especially at higher temperature as elucidated in Fig. 6.

3.3. Quasi-static properties

The average tensile engineering stress v. engineering strain responses of neat polyurea and Polyurea-Polyurea composite are shown in Fig. 7a based on averaging the data acquired from testing five samples at quasi-static loading condition. Regardless of the sample type, the stress-strain behavior can be characterized to exhibit large strains at level of several hundreds percentage of strain, but the composite samples show a distinctively different mechanical response that can be described as an elasto-plastic behavior given the initial linear dependence of the stress-strain while by nearly constant stress while the strain is monotonically increasing. On the other hand, the bulk samples showed generally nonlinear response starting by a relatively narrow region of linear elasticity followed by a large stress plateau and ending with a region where the stress of the samples started to flow. Since the neat polymer samples reached flow stress, it exhibits a notable plastic strain. That is, the permanent plastic strain in the neat polyurea sample is shown to be substantially larger than the Polyurea-Polyurea composite sample, where the former was reported to fail at ~976 % strain while the latter failed at ~600 % strain as shown in Fig. 7a. Examples of the failed samples are also included in Fig. 7b, which provides qualitative evidence for the changes in the stress-strain behavior of the samples with and without the polyurea microspheres reinforcement.

To quantitatively study the difference in the behavior between the quasi-static response of neat polyurea and Polyurea-Polyurea composite samples, several mechanical properties including the elastic modulus (E), toughness (U), yield stress (Y_0), and strain at failure (ϵ_f) were calculated and collated in Table 1. While the elastic modulus, toughness, and strain at failure are calculated based on their traditional definition, the yield stress is defined as by the offset method. As can be deduced from Table 1, the elastic modulus remained nearly unchanged when comparing the bulk (51.56 ± 7.42 MPa) and composite (51.95 ± 3.74 MPa) samples, which is attributed to the relatively low weight percentage of the reinforcing microspheres as well as due to the matrix dominated response as discussed before. On the other hand, there is a significant difference between the remaining metrics, namely yield, toughness and strain to failure. The 0.2 % yield stress of the Polyurea-Polyurea composite (2.77 ± 0.26 MPa) was found, on average to increase by 40 % over that of neat polyurea (1.98 ± 0.22 MPa). Finally, the toughness and strain at failure showed higher sensitivity to polyurea microspheres, where the former was nearly reduced by 62 % and the latter cut by 55 % as shown by the numbers included in Table 1. The reductions in toughness and strain at failure are attributed to the inclusion of the stiffer polyurea microspheres, which act as pinning sites resulting in strain localization and premature failure in the surrounding matrix.

To better elucidate the difference in the mechanical behavior between reinforced and neat polyurea samples, the fracture surfaces of failed samples after quasi-static testing were observed under the scanning electron microscope. The SEM micrograph of the bulk polyurea sample shown in Fig. 8a indicates that the sample exhibited ductile failure, where the uniaxial tensile stress evolved at intrinsic shearing planes within the samples resulting in tearing at nearly the middle of the gauge length. On the other hand, the fracture surfaces of Polyurea-

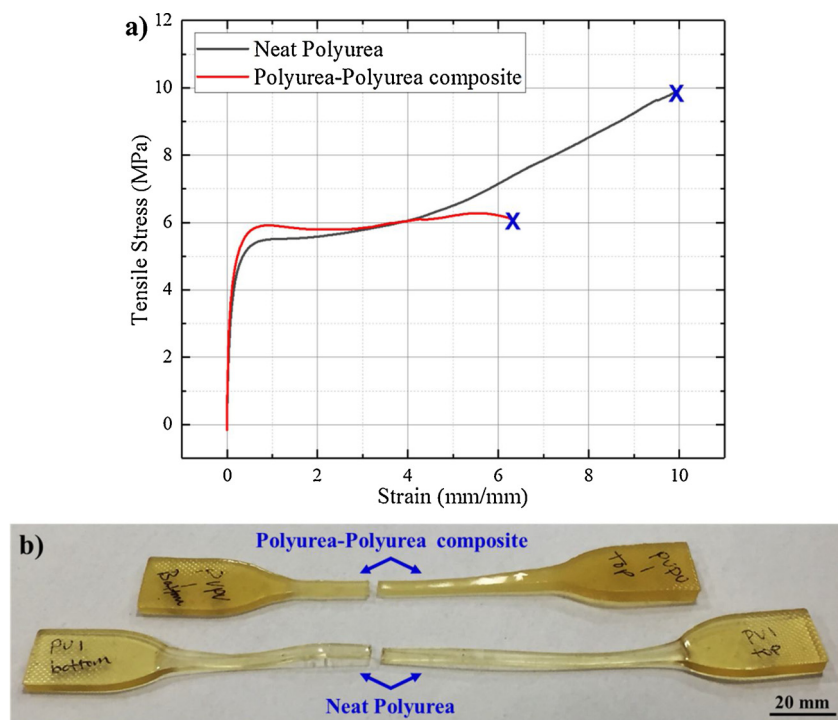


Fig. 7. (a) Average stress-strain behavior for Polyurea-Polyurea composite and Neat Polyurea based on quasi-statically testing five samples and (b) the final geometry of the samples after failure showing the polyurea-polyurea composite exhibiting lower permanent deformation than its neat counterpart.

Table 1
Quasi-Static Tensile Properties of Neat Polyurea and Polyurea-Polyurea composite.

Material	E (MPa)	U (MPa)	γ_0 (MPa)	ε_f
Neat	51.56 ± 7.42	66.89 ± 6.01	1.98 ± 0.22	9.76 ± 0.65
Composite	51.95 ± 3.74	25.16 ± 8.22	2.77 ± 0.26	4.35 ± 1.29

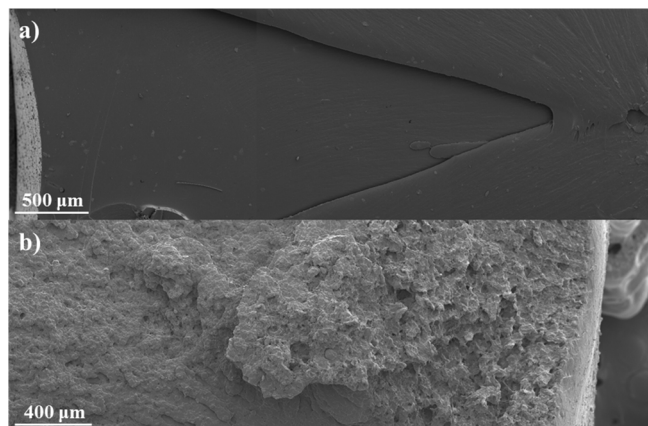


Fig. 8. SEM micrograph of a) the Neat Polyurea sample showing the evolution of shear planes due to the axial loading and b) the Polyurea-Polyurea composite at the site of failure demonstrating the brittle-like fracture surface due to the effect of microspheres in creating pinning-sites for strain localization.

Polyurea composite samples are characterized as localized rough surfaces, which is associated with strain localization due to the disparity in the stiffness between the microspheres and the adjacent compliant matrix. In other words, the stress tends to build-up due to the mismatch in the elastic properties, which in turn exceeds the strength of the polyurea matrix resulting in a matrix dominated failure, as discussed above. Further examination of the fracture surface of the Polyurea-

Polyurea composite sample points to the nature of the failure as a cohesion failure rather than an adhesion failure since there were no fractured microspheres observed. In short, the stiff polyurea microspheres acted as pinning sites preventing shear deformation from sliding and unkinking of the macromolecule chains, hence resulting in failure due to strain localization in the vicinity of the microspheres.

Overall, the use of polyurea microspheres as a reinforcement material in a polyurea matrix was shown to maintain the hydrothermal stability found in the bulk material, increase the elastic modulus in micro-scale compression testing, slightly increase the compliance of the material in dynamic mechanical testing, but weaken the material in quasi-static tensile testing.

4. Conclusion

In summary, the Polyurea-Polyurea composite was successfully synthesized and the microspheres were shown to be well dispersed within the polyurea matrix after close examination of the SEM micrographs. When tested at the microscale, the addition of microspheres enhanced the stiffness, with the composite having an average stiffness of 35.83 ± 12.78 MPa. Through dynamic mechanical testing, the addition of microspheres was found to slightly enhance the compliance of the composite, depending on the temperature. The creep strains at temperatures above glass transition were found to increase, while below T_g decreased due to the addition of polyurea microspheres, where the latter acted as pinning sites that hindered the intermolecular motion. From quasi-static tensile testing, it was found that the addition of the microspheres negatively affected the elongation of the sample and altered its stress-strain behavior. The interfacial bonding between the microspheres and the surrounding polyurea matrix was optimal due to mechanical interlocking and chemical bonding. Nonetheless, the composite samples exhibited mechanical failure at lower stresses than their near counterparts. In all, the newly formulated composite will be further researched using in-situ characterization techniques to further elucidate the evolution of the microstructure as a function of reinforcement volume fraction and loading conditions. The Polyurea-

Polyurea composite reported herein may be suitable for novel modular armor and protective coatings.

Data availability

The data required to reproduce these findings are available upon request. Interested researchers are encouraged to contact the corresponding author.

Declaration of Competing Interest

The authors declare that they have no known competing financial interests or personal relationships that could have appeared to influence the work reported in this paper.

Acknowledgements

The research leading to these results was supported in part by the United States Department of Defense under Grant Agreement No. W911NF-14-1-0039 and W911NF-18-1-0477. The research was also supported by internal funds from San Diego State University. The authors also acknowledge the use of equipment at the San Diego State University Electron Microscopy Facility acquired by NSF instrumentation grant DBI-0959908 and award No. 1925539.

Appendix A. Supplementary data

Supplementary material related to this article can be found, in the online version, at doi:<https://doi.org/10.1016/j.mtcomm.2020.101464>.

References

[1] J. Aboudi, S.M. Arnold, B.A. Bednarcyk, *Micromechanics of Composite Materials: A Generalized Multiscale Analysis Approach*, Butterworth-Heinemann, 2012.

[2] S. Newacheck, G. Youssef, Synthesis and characterization of polarized novel 0-3 Terfenol-D/PVDF-TrFE composites, *Compos. Part B Eng.* 172 (2019) 97–102, <https://doi.org/10.1016/j.compositesb.2019.05.043>.

[3] G. Youssef, G. Pessoa, S. Nacy, Effect of elevated operating temperature on the dynamic mechanical performance of E-glass/epoxy composite, *Compos. Part B Eng.* 173 (2019) 106937, <https://doi.org/10.1016/j.compositesb.2019.106937>.

[4] W.D.C. Jr, D.G. Rethwisch, *Fundamentals of Materials Science and Engineering: An Integrated Approach*, John Wiley & Sons, 2012.

[5] E.-M. Rosenbauer, K. Landfester, A. Musyanovich, Surface-active Monomer as a stabilizer for polyurea nanocapsules synthesized via interfacial polyaddition in inverse miniemulsion, *Langmuir* 25 (2009) 12084–12091, <https://doi.org/10.1021/la9017097>.

[6] T. Ahamad, V. Kumar, N. Nishat, New class of anti-microbial agents: synthesis, characterization, and anti-microbial activities of metal chelated polyurea, *J. Biomed. Mater. Res. Part A* 88A (2009) 288–294, <https://doi.org/10.1002/jbma.a.31872>.

[7] V. Gupta, J.K. Citron, G. Youssef, Material for mitigating impact forces with collision durations in nanoseconds to milliseconds range, US Patent 13/879,616, 2013.

[8] V. Gupta, G. Youssef, Orientation-dependent impact behavior of Polymer/EVA bilayer specimens at long wavelengths, *Exp. Mech.* 54 (2014), <https://doi.org/10.1007/s11340-014-9854-6>.

[9] A. Jain, G. Youssef, V. Gupta, Dynamic tensile strength of polyurea-bonded steel/E-glass composite joints, *J. Adhes. Sci. Technol.* 27 (2013).

[10] H. Kim, J. Citron, G. Youssef, A. Navarro, V. Gupta, Dynamic fracture energy of polyurea-bonded steel/E-glass composite joints, *Mech. Mater.* 45 (2012) 10–19, <https://doi.org/10.1016/j.mechmat.2011.08.017>.

[11] G.S. Barsoum, P.J. Dudit, The fascinating behaviors of ordinary materials under dynamic conditions, *Ammtiac Quart.* 4 (2002) 11–14.

[12] R.G.S. Barsoum, *Elastomeric Polymers With High Rate Sensitivity: Applications in Blast, Shockwave, and Penetration Mechanics*, William Andrew, (2015).

[13] R. Casalini, R. Bogoslov, S.B. Qadri, C.M. Roland, Nanofiller reinforcement of elastomeric polyurea, *Polymer* 53 (2012) 1282–1287, <https://doi.org/10.1016/j.polymer.2012.01.034>.

[14] E.I. Akpan, X. Shen, B. Wetzel, K. Friedrich, 2 - design and synthesis of polymer nanocomposites, in: K. Pielichowski, T.M. Majka (Eds.), *Polymer Composites With Functionalized Nanoparticles*, Elsevier, 2019, pp. 47–83, , <https://doi.org/10.1016/B978-0-12-814064-2.00002-0>.

[15] G. B, Z. D, L. B, Y. P, L. P, Polyvinyl alcohol microspheres reinforced thermoplastic starch composites, *Materials (Basel)* 11 (2018), <https://doi.org/10.3390/ma11040640>.

[16] S. Do, Synthesis and Characterization of Polyurea-Polyurea Composite, San Diego State University, 2018, <https://search.proquest.com/openview/73f7ef28c0be7bfdf237c913ff315c9e/1?pq-origsite=gscholar&cbl=18750&diss=y>.

[17] J. Xu, H. Han, L. Zhang, X. Zhu, X. Jiang, X.Z. Kong, Preparation of highly uniform and crosslinked polyurea microspheres through precipitation copolymerization and their property and structure characterization, *RSC Adv.* 4 (2014) 32134–32141, <https://doi.org/10.1039/C4RA04206A>.

[18] I. Whitten, G. Youssef, The effect of ultraviolet radiation on ultrasonic properties of polyurea, *Polym. Degrad. Stab.* 123 (2016) 88–93, <https://doi.org/10.1016/j.polymdegradstab.2015.11.009>.

[19] G. Youssef, J. Brinson, I. Whitten, The effect of ultraviolet radiation on the hyperelastic behavior of polyurea, *J. Polym. Environ.* 26 (2018) 183–190, <https://doi.org/10.1007/s10924-016-9033-x>.

[20] G. Youssef, I. Whitten, Dynamic properties of ultraviolet-exposed polyurea, *Mech. Time-Depend. Mater.* 21 (2017) 351–363, <https://doi.org/10.1007/s11043-016-9333-9>.

[21] A.M. Shaik, N.U. Huynh, G. Youssef, Micromechanical behavior of ultraviolet-exposed polyurea, *Mech. Mater.* 140 (2020) 103244, <https://doi.org/10.1016/j.mechmat.2019.103244>.

[22] J. Zhao, W.G. Knauss, G. Ravichandran, Applicability of the time-temperature superposition principle in modeling dynamic response of a polyurea, *Mech. Time-Depend Mater.* 11 (2007) 289–308, <https://doi.org/10.1007/s11043-008-9048-7>.

[23] W.C. Oliver, G.M. Pharr, An improved technique for determining hardness and elastic modulus using load and displacement sensing indentation experiments, *J. Mater. Res.* 7 (1992) 1564–1583.

[24] R.M. Christensen, *Mechanics of Composite Materials*, (2005).

[25] S. Ebnesajjad, 4 - surface and material characterization techniques, in: S. Ebnesajjad (Ed.), *Surface Treatment of Materials for Adhesion Bonding*, William Andrew Publishing, Norwich, NY, 2006, pp. 43–75, , <https://doi.org/10.1016/B978-081551523-4.50006-7>.

[26] J. Qiao, A.V. Amirkhizi, K. Schaaf, S. Nemat-Nasser, G. Wu, Dynamic mechanical and ultrasonic properties of polyurea, *Mech. Mater.* 43 (2011) 598–607, <https://doi.org/10.1016/j.mechmat.2011.06.012>.